

■ **CARTILAGE**

# Rejuvenated ageing mesenchymal stem cells by stepwise preconditioning ameliorates surgery-induced osteoarthritis in rabbits

**Z. Zong,  
X. Zhang,  
Z. Yang,  
W. Yuan,  
J. Huang,  
W. Lin,  
T. Chen,  
J. Yu,  
J. Chen,  
L. Cui,  
G. Li,  
B. Wei,  
S. Lin**

From Affiliated Hospital of Guangdong Medical University, Zhanjiang, China

**Aims**

Ageing-related incompetence becomes a major hurdle for the clinical translation of adult stem cells in the treatment of osteoarthritis (OA). This study aims to investigate the effect of stepwise preconditioning on cellular behaviours in human mesenchymal stem cells (hMSCs) from ageing patients, and to verify their therapeutic effect in an OA animal model.

**Methods**

Mesenchymal stem cells (MSCs) were isolated from ageing patients and preconditioned with chondrogenic differentiation medium, followed by normal growth medium. Cellular assays including Bromodeoxyuridine / 5-bromo-2'-deoxyuridine (BrdU), quantitative polymerase chain reaction (q-PCR),  $\beta$ -Gal, Rosette forming, and histological staining were compared in the manipulated human mesenchymal stem cells (hM-MSCs) and their controls. The anterior cruciate ligament transection (ACLT) rabbit models were locally injected with two millions, four millions, or eight millions of hM-MSCs or phosphate-buffered saline (PBS). Osteoarthritis Research Society International (OARSI) scoring was performed to measure the pathological changes in the affected joints after staining. Micro-CT analysis was conducted to determine the microstructural changes in subchondral bone.

**Results**

Stepwise preconditioning approach significantly enhanced the proliferation and chondrogenic potential of ageing hMSCs at early passage. Interestingly, remarkably lower immunogenicity and senescence was also found in hM-MSCs. Data from animal studies showed cartilage damage was retarded and subchondral bone remodelling was prevented by the treatment of preconditioned MSCs. The therapeutic effect depended on the number of cells applied to animals, with the best effect observed when treated with eight millions of hM-MSCs.

**Conclusion**

This study demonstrated a reliable and feasible stepwise preconditioning strategy to improve the safety and efficacy of ageing MSCs for the prevention of OA development.

**Cite this article:** *Bone Joint Res* 2021;10(1):10–21.

**Keywords:** Osteoarthritis, Mesenchymal stem cell, Chondrogenic differentiation, Ageing cell

**Article focus**

■ We presented a stepwise preconditioning method which successfully rejuvenated stemness of ageing human mesenchymal stem cells (hMSCs).

■ Intra-articular administration of a single dose of the resulted mesenchymal stem cells (MSCs) ameliorated osteoarthritis (OA) phenotypes in rabbits.

Correspondence should be sent to Sien Lin; email: sienlin@stanford.edu

doi: 10.1302/2046-3758.101.BJR-2020-0249.R1

*Bone Joint Res* 2021;10(1):10–21.

### Key messages

- Cell proliferation, viability, immunogenicity, and chondrogenic differentiation potential of the MSCs from ageing patients after stepwise preconditioning were significantly improved.
- Dose-dependent administration of MSCs after stepwise preconditioning ameliorated surgery-induced OA by retarding cartilage destruction and preventing subchondral bone from remodelling.

### Strengths and limitations

- The strength of this study is its novel approach in employing a stepwise preconditioning method to rejuvenate ageing hMSCs.
- The main limitation of this study is a lack of evidence to show the effects of the control hMSCs *in vivo*.

### Introduction

Osteoarthritis (OA) is a common musculoskeletal morbidity and one of the leading causes of disability worldwide.<sup>1</sup> OA affects nearly 80% of people aged older than 70 years in the USA.<sup>2</sup> Asian countries such as China face the same situation, with a remarkable increase in the number of OA patients due to a rapidly ageing population.<sup>3</sup> Although there are numerous nonoperative, non-pharmacological, and pharmacological treatments which may help to control patients' symptoms including pain, stiffness, and effusion, the current strategies are incapable of reversing the damaged joint.<sup>4</sup> Operative interventions including microfracture, mosaicplasty, and fresh osteochondral allograft (FOCA) are available although limitations exist.<sup>5</sup> Total joint replacement (TJR) is recommended as the final option to regain reasonable function of joint movement at the expense of potential surgical complications, as per the recently released consensus on OA managements.<sup>6</sup>

During the last two decades, the rapid development of regenerative medicine provides potential breakthroughs for cartilage repair. As the first cell-based regenerative medicine approach, autologous chondrocyte implantation (ACI) has emerged as an effective and durable solution for the treatment of large full-thickness cartilage and osteochondral lesions of the knee joint.<sup>7</sup> However, many hurdles such as donor site morbidity and chondrocyte dedifferentiation in cell cultures limit the wide acceptance of ACI.<sup>8,9</sup> Stem cell-based regenerative medicine represents one of the most attractive directions of modern medicine due to its pluripotency of proliferation, differentiation, and immunomodulation. Mesenchymal stem cells (MSCs) reside in various tissues and expand easily in cultures, which make them important "seed cells" for cartilage regeneration.<sup>9-11</sup> However, MSC-based therapy also faces many obstacles to be overcome before it can be applied generally in clinical settings. Firstly, the quality of MSCs may vary greatly in different donors with different ages and

health status; MSCs from ageing patients are usually less potent than younger ones.<sup>12,13</sup> Secondly, adult MSCs have a limited lifespan in many patients. After a certain number of cell divisions, MSCs enter replicative senescence, which is morphologically characterized by enlarged and irregular cell shapes and ultimately a halt to proliferation and differentiation.<sup>14</sup> There is a high demand to attain MSCs with a stable genotype and phenotype for cell therapy in OA.

Recent studies have attempted to apply stepwise chondrogenic preconditioning using chondrogenic differentiation medium followed by normal growth medium to improve the stemness of MSCs.<sup>15,16</sup> Lin et al<sup>15</sup> reported that not only could chondrogenic differentiation potential be considerably enhanced, but also that cell proliferation and anti-apoptosis could be greatly improved in MSCs, with the mechanism related to epigenetic modifications in pluripotent markers. Animal studies confirmed the preconditioned MSCs took advantage of retarding cartilage damage in an OA rat model and promoted cartilage healing in an osteochondral defect rat model.<sup>15,16</sup> Hence, it is of clinical interest to investigate the cellular behaviours of human mesenchymal stem cells (MSCs) augmented by stepwise preconditioning. This study was designed to further investigate such cellular behaviours, including proliferation, chondrogenic differentiation, cellular senescence, and immunogenicity. Further, an anterior cruciate ligament transection (ACLT) rabbit model was established to examine the safety and efficacy of the preconditioned hMSCs *in vivo*.

### Methods

**Collection of human marrow and blood samples.** The study was carried out at Affiliated Hospital of Guangdong Medical University, Zhanjiang, China. Human bone marrow was obtained from patients ( $n = 3$ , all male, mean age 64.3 years (SD 6.8)) and underwent arthroplasty due to hip fracture in accordance with The Code of Ethics of the World Medical Association (Declaration of Helsinki) for experiments involving humans.<sup>17</sup> Patients with liver or renal function failure, hormone disorders, diabetes mellitus, a history of neurological impairment, and those who had taken glucocorticoid medications were excluded. Peripheral blood was also harvested from the same patients for isolation of lymphocytes. Procedures involved in cell harvesting and culturing were approved by the Clinical Research Ethical Committee of Affiliated Hospital of Guangdong Medical University, and informed consent was obtained from the patients prior to the experiments.

**Isolation and characterization of human bone marrow-derived MSCs.** Bone marrow (BM) nucleated cells were harvested as described in previous studies.<sup>18,19</sup> In brief, the fractured femoral head was removed by the surgeons (JC and BW) before harvesting the BM from the femoral shaft. Using aseptic techniques, BM samples

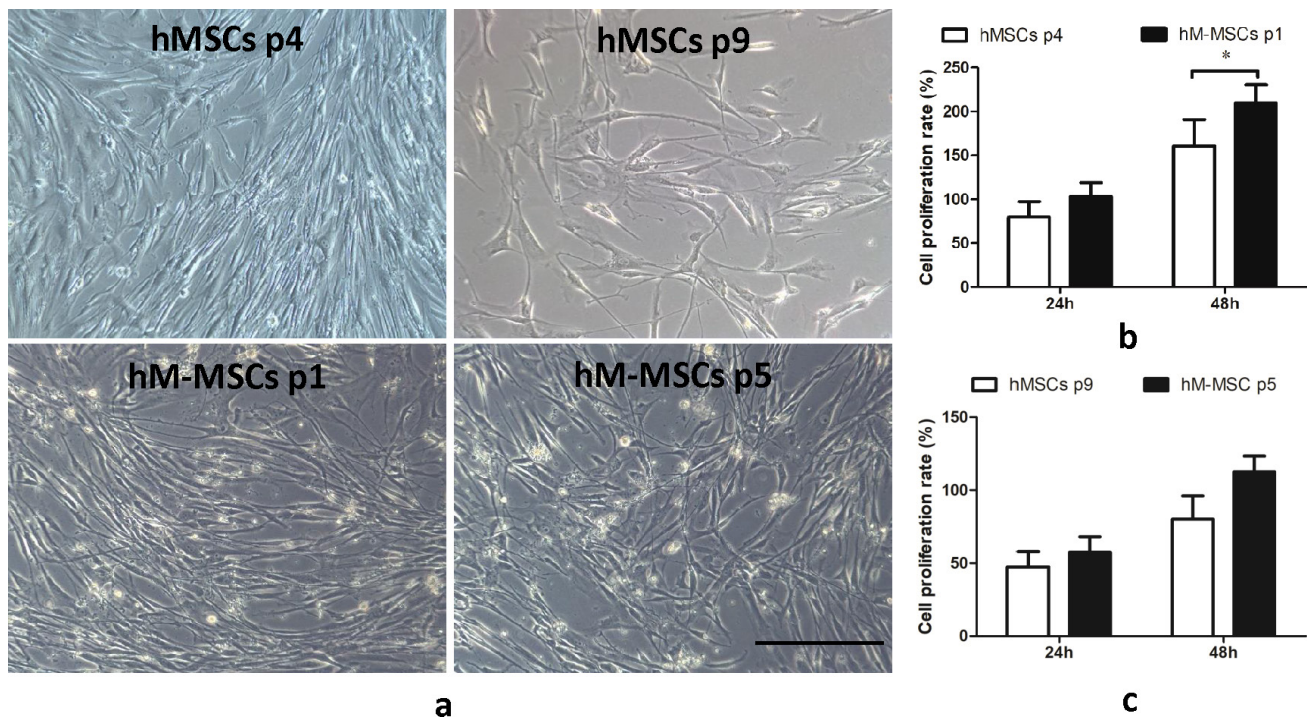


Fig. 1

Cell morphology and proliferation of manipulated human mesenchymal stem cells (hM-MSCs) and their untreated human mesenchymal stem cells (hMSCs) controls. a) Cell morphology of hM-MSCs (passage 1 or 5) and their untreated hMSCs controls (passage 4 or passage 9). b) Cell proliferation rate of hM-MSCs at passage 1 (p1) and their untreated hMSCs controls (hMSCs p4) measured at 24 hours or 48 hours after culture by Bromodeoxyuridine / 5-bromo-2'-deoxyuridine (BrdU) assay. c) Cell proliferation of hM-MSCs at passage 5 (p5) and their untreated hMSCs controls (hMSCs p9) measured at 24 hours or 48 hours after culture by BrdU assay. The representative images shown were derived from the bone marrow of donor 1. The data are expressed as mean and SD ( $n = 2$  donors with three replicates for each donor). \* $p < 0.05$  versus human mesenchymal stem cells (MSCs) controls. Scale bar: 50  $\mu\text{m}$ .

were harvested and transferred to cell culture lab immediately in cold phosphate-buffered saline (PBS) on ice. The samples were cut into small pieces and digested by 0.22% Collagenase solution (Sigma-Aldrich, St Louis, Missouri, USA). After filtering through the 70  $\mu\text{m}$  nylon mesh (Corning, Durham, North Carolina, USA), the cells were washed and then treated with red blood cells lysis buffer (BioLegend, San Diego, California, USA). Nucleated cells were plated at  $10^4$  cell/ $\text{cm}^2$  and cultured in modified Eagle's medium of  $\alpha$  ( $\alpha$ -MEM; Thermo Fisher Scientific, Waltham, Massachusetts, USA) supplemented with 10% fetal bovine serum (FBS; Thermo Fisher Scientific), and 1% penicillin-streptomycin (PS) antibiotic mixture (Thermo Fisher Scientific) at 37°C with 5%  $\text{CO}_2$  and 95% humidity. The culture medium was changed every three days. The cells from passages 3 to 6 were used in further experiments. The purity of hMSCs was determined by flow cytometry and lineage differentiation potential including osteogenesis, adipogenesis, and chondrogenesis as described elsewhere in the literature.<sup>20</sup> Human MSCs were successfully isolated and expanded for further experiments from two out of the three donors.

**Cells preconditioning and cell proliferation.** MSCs from BM were manipulated by stepwise preconditioning with chondrogenic differentiation induction medium, followed by normal growth medium.<sup>15,16</sup> Briefly, the

hMSCs were primed with chondrogenic differentiation induction medium (CIM) consisting of Dulbecco's modified Eagle's medium (DMEM) supplied with 100 nM dexamethasone, 40 mg/ml proline, 10 ng/ml transforming growth factor- $\beta$ 1 (PeproTech, Rocky Hill, New Jersey, USA), and 50 mg/ml ascorbate-2-phosphate for seven days. After chondrogenic induction for seven days (induction phase), the medium was replaced by normal growth medium ( $\alpha$ -MEM) and cultured for another seven days (expansion phase). The resulted manipulated human mesenchymal stem cells (hM-MSCs) were used for further experiments. Beginning from the expansion phase, the untreated hMSCs at the passage of 3 were cultured with normal growth medium ( $\alpha$ -MEM) as the controls of hM-MSCs. Cell morphology, chondrogenic differentiation, immune response, and cell senescence of the cells hMSCs and hM-MSCs were determined after they were subcultured either once more or an additional five times. After the prime step, the passage of hM-MSCs was regarded as 0. After being subcultured once, the passage was regarded as p1, and so forth. Cell proliferation of hM-MSCs (passage 1 or 5) and their hMSCs controls (passage 4 or passage 9) was measured by the BrdU assay (Roche Applied Science, Indianapolis, Indiana, USA) after 24 hours or 48 hours of cell culture. Cell proliferation rate was determined by the Optical Density (OD) values measured after 24 hours or 48



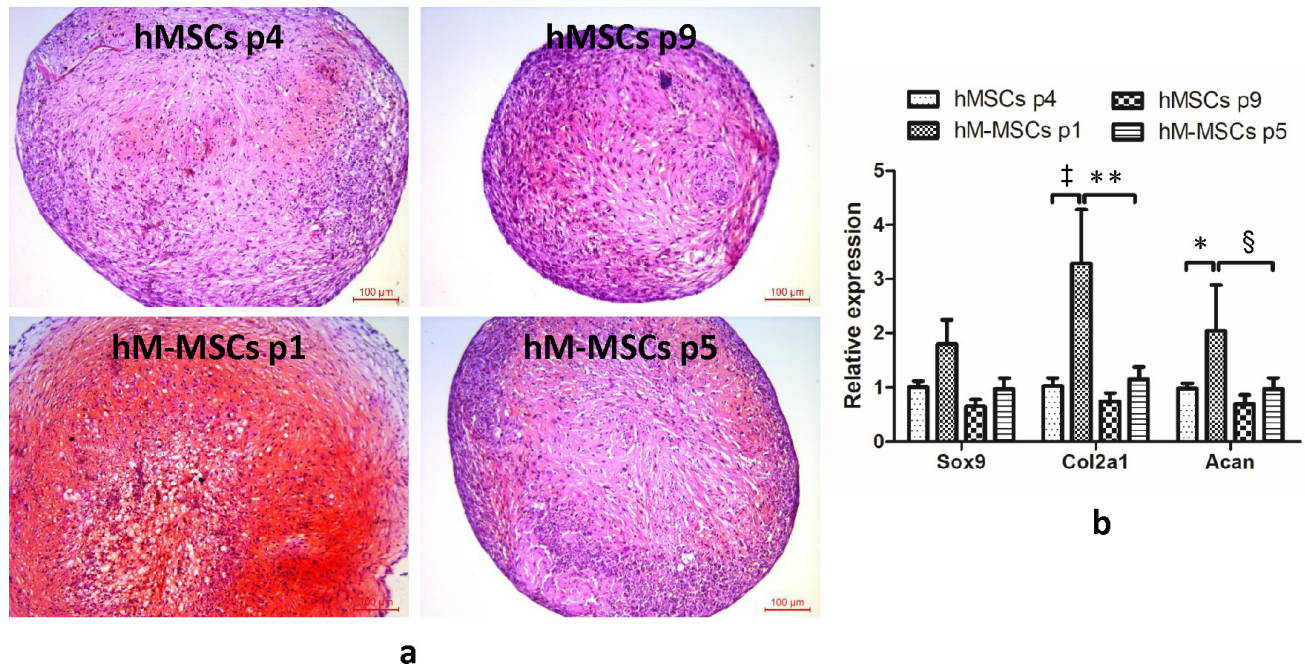


Fig. 2

Chondrogenic differentiation capacity of manipulated human mesenchymal stem cells (hM-MSCs) (passage 1 or 5) and their untreated human mesenchymal stem cells (hMSCs) controls (passage 4 or passage 9). a) Safranin O staining results of hM-MSCs or untreated hMSCs controls. b) Relative expression of chondrogenic differentiation markers including Sox9, Col2a1, and Aggrecan (Acan) in hM-MSCs or untreated hMSCs controls. The representative images shown were derived from the bone marrow of donor 1. The data are expressed as mean and SD ( $n = 2$  donors with three replicates for each donor).  $^{\dagger}p < 0.05$ ,  $^{\ddagger}p < 0.001$  versus human mesenchymal stem cells (hMSCs) controls.  $^{\S}p < 0.05$ ,  $^{**}p < 0.001$  versus hM-MSCs at passage 1 (hM-MSCs p1).

hours of cell culture normalized by the mean values measured at the beginning (0 hours) of cell culture.

**Chondrogenic differentiation.** To compare chondrogenic differentiation potential, hM-MSCs (p1 or p5) or hMSCs (p4 or p9) controls were subjected to cell pellet culture. In total,  $5 \times 10^5$  cells (hM-MSCs or hMSCs) were centrifuged to form pellets and cultured in CIM. The medium was changed every three days. Total RNA was extracted with Trizol (Thermo Fisher Scientific) at day 7 for quantitative real-time polymerase chain reaction (qRT-PCR). At day 21, the cell pellets were fixed with 4% buffered formaldehyde (Sigma-Aldrich) for further histological analysis.

**Rosette formation assay.** Mixed lymphocyte culture was performed to examine the immune response of resting human peripheral blood lymphocytes (hPBLs) to hMSCs and hM-MSCs.<sup>21</sup> Briefly, hPBLs were isolated from peripheral blood. The PBLs were used for cell membrane labeling with PKH26 (red) Fluorescent Cell Linker Kits (Sigma-Aldrich). Manipulated hMSCs (p1 or p5) or hMSCs (p4 or p9) controls were labelled with PKH67 (green) Fluorescent Cell Linker Kits (Sigma-Aldrich). After being labelled with different kinds of dyes, hPBLs and hMSCs or hPBLs and hM-MSCs were pipetted into the chamber slides (Thermo Fisher Scientific) in a density of  $1 \times 10^6/\text{cm}^2$  and  $1 \times 10^4/\text{cm}^2$  for cell culturing, respectively. Once co-cultured with complete medium for three days, the unattached cells were washed out and the remaining

cells in the culture were visualized using a Leica TCS SP8 confocal microscope (Leica, Wetzlar, Germany). Human PBLs formed rosette rings around co-cultured hMSCs or hM-MSCs, which were then counted with a haemocytometer. Binding rate was calculated as hPBLs binding hMSCs or hM-MSCs ( $> 10$  hPBLs binding to one hMSC or hM-MSC) to the total number of hMSCs or hM-MSCs in five random spots in each well ( $n = 3$  for each donor).

**Senescence-associated beta-galactosidase assay.** Cellular senescent status of hM-MSCs (p1 or p5) or hMSCs (p4 or p9) controls was determined by senescence-associated beta-galactosidase (SA- $\beta$ -gal) assay.<sup>20,22</sup> The expression of SA- $\beta$ -gal at cellular level was determined with a commercial staining kit (Cell Signalling, Danvers, Massachusetts, USA) according to the manufacturer's instruction. In brief, cells grown on six-well plates were fixed with fixative solution for 15 minutes, washed twice with PBS, stained with 1 ml freshly prepared staining solution, and incubated overnight at 37 °C. The quantification of SA- $\beta$ -gal activity was conducted with SA- $\beta$ -gal Assay Kit (Thermo Fisher Scientific) according to the instruction. Cells were lysed with two freezing and thawing cycles with liquid nitrogen and 37°C water bath. The cell lysate then reacted with o-nitrophenyl- $\beta$ -D-galactopyranoside at 37°C and the absorbance at 420 nm was measured as indicated by the relative activity of SA- $\beta$ -gal.

**Gene expression.** After chondrogenic differentiation for seven days, total RNA from human cells was extracted

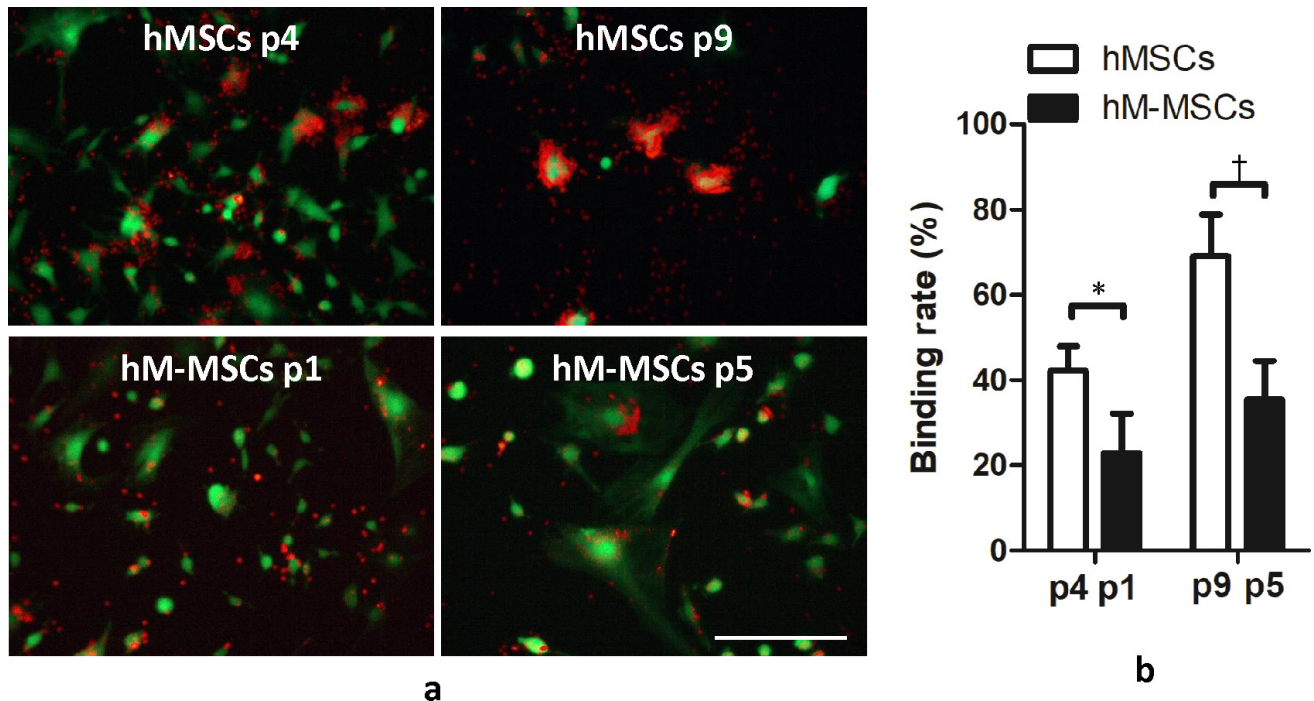


Fig. 3

Coculture of human peripheral blood lymphocytes (hPBLs) and manipulated human mesenchymal stem cells (hM-MSCs) (passage 1 or 5) or their untreated human mesenchymal stem cells (hMSCs) controls (passage 4 or passage 9) tested by Rosette forming assay. a) PKH26-labelled (red) stained PBLs formed rosette rings around PKH67-labelled (green) stained hM-MSCs. b) PBL binding rate of hMSCs controls or hM-MSCs. Binding rate was calculated as hPBLs binding hMSCs or hM-MSCs (> ten hPBLs binding to one hMSC or hM-MSC) to the total number of hMSCs or hM-MSCs in five random spots. The representative images shown were derived from the bone marrow of donor 1. The data are expressed as mean and SD (n = 2 donors with three replicates from each donor). \*p < 0.05, †p < 0.01 versus human mesenchymal stem cells (hMSCs) controls. Scale bar: 50  $\mu$ m.

using Trizol (three replicates for each group) to perform real-time quantitative reverse transcription (qRT-PCR). Total RNA was used as the template to reverse transcribe complementary DNA (cDNA) using Prime Script RT Enzyme mix (Takara, Kusatsu, Japan). Quantitative real-time polymerase chain reaction (qPCR) was performed with Power SYBR Green PCR Master Mix (Thermo Fisher Scientific) by Step-One-Plus Real Time PCR Systems (Thermo Fisher Scientific) and glyceraldehyde 3-phosphate dehydrogenase (GAPDH) expression was used as internal control. Primer sequences were determined by GenBank sequences. The sequences are listed below: GAPDH forward: 5'AGGGCTGCTTTAACTCTGGTAAA3', reverse: 5'GAATTTGCCATGGGTGGAAT 3'; Sox9 forward: 5'CAGAACACCAGCAGTTAA3', reverse: 5'AACAACAGATGACCATACC3'; Aggrecan (Acan) forward: 5' CAGAATCAACTGCTGCAGACCA3', reverse: 5' TTCGATGGTCTGTGCTTCAG3'; Collagen type II  $\alpha$ 1 (Col 2a1) forward: 5'GGCAATAGCAGGTTACAGTACA3', reverse: 5'CGATAACAGTCTTGCCCCACTT3'.

**Animal surgeries and sample collection.** The efficiency of cell therapy by using hM-MSCs for the treatment of surgery-induced OA was determined by animal experiment. In order to gain sufficient number of cells for animal study, the cells from two donors were pooled with a ratio of 1:1 before injection. The hM-MSCs used in the animal experiments were from passage 2 to 3. Animal

experimental protocol was modified according to previous reports.<sup>11,15</sup> In all, 20 male New Zealand white rabbits weighing a mean of 3.3 kg (SD 0.5) were anaesthetized by 10% ketamine mixed with 2% xylazine. After disinfection, the anterior cruciate ligament (ACL) of the right knee of each rabbit was exposed after dislocating the medial parapatellar. The knee was placed in full flexion and cut with care using a scalpel, avoiding damage to the articular cartilage. The joint capsule, subcutaneous tissue, and skin were closed with sutures after the medial parapatellar relocated. Animals were then housed in their individual cages in a clean and controlled environment, with free access to food and water. After 14 days postoperatively, the rabbits were injected once with 100  $\mu$ l PBS (OA+ PBS controls, n = 5), two millions of hM-MSCs (OA+ hM-MSCs-L, n = 5), four millions of hM-MSCs (OA+ hM-MSCs-M, n = 5), or eight millions of hM-MSCs (OA+ hM-MSCs-H, n = 5), respectively, in 100  $\mu$ l PBS into the right knee joint with a 25G syringe under isoflurane anaesthesia. The local temperature of the knee skin was monitored by an infrared thermometer (JEWY Tech, Shenzhen, China). The right knees were harvested eight weeks after cell therapy. The contralateral left knees were also collected as intact controls.

**3D microstructural analysis.** Subchondral bone microstructure under medial side of tibial plateaus was determined by high-resolution micro-CT 40 system scans



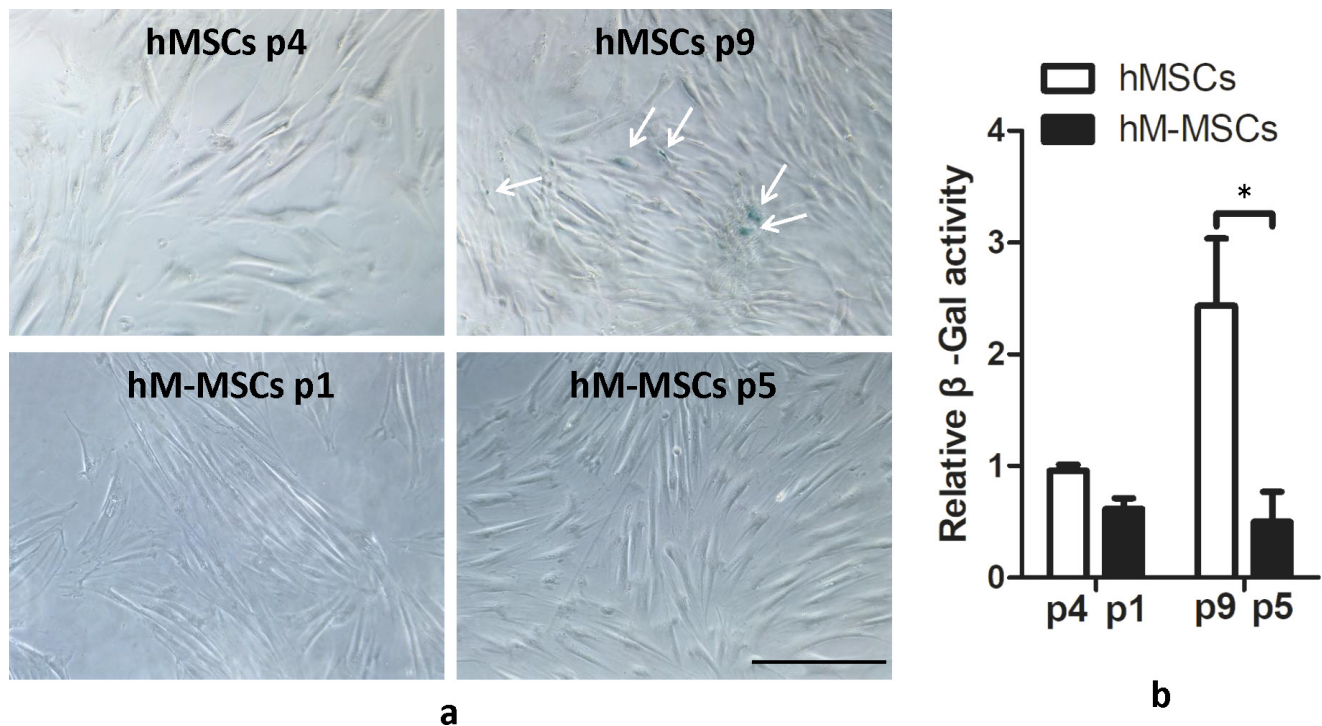


Fig. 4

Senescence-associated beta-galactosidase (SA- $\beta$ -gal) activity in manipulated human mesenchymal stem cells (hM-MSCs) (passage 1 or 5) or their untreated human mesenchymal stem cells (hMSCs) controls (passage 4 or passage 9). a) Results of SA- $\beta$ -gal staining examined by bright field microscopy. White arrows point to the  $\beta$ -gal positive-stained cells. b) Quantitative results of SA- $\beta$ -gal activity in cell lysis. The representative images shown were derived from the bone marrow of donor 1. The data are expressed as mean and SD ( $n = 2$  donors with three replicates from each donor). \* $p < 0.01$  versus hMSCs controls. Scale bar: 50  $\mu$ m.

(Scanco Medical, Wangen-Brüttisellen, Switzerland). Besides the total subchondral bone, trabecular bone compartment was also segregated by selecting the region of interest at the cancellous bone and excluding the subchondral plate and the calcified growth plate. A total of 100 3D sagittal images of the tibiae medial subchondral bone ( $n = 5$ ) were evaluated at global threshold (158 mg hydroxyapatite/cm<sup>3</sup>) and a Gaussian filter was used (sigma: 0.8, support: 2) to suppress image noise. Parameters including bone mineral density (BMD) and bone volume/total tissue volume (BV/TV) were determined with a built-in program (Image Processing Language v4.29d, Scanco Medical).<sup>15,23</sup>

**Histological analysis.** After micro-CT scanning, the knee joints ( $n = 5$  per group) were decalcified and paraffin-embedded for histological analysis. Then 5  $\mu$ m thickness sections were subjected to Safranin O and Fast Green staining or hematoxylin and eosin (H&E) staining (all chemicals purchased from Sigma-Aldrich). The Osteoarthritis Research Society International (OARSI) OA scoring system was adopted to analyze the pathological changes in the joint as previously described.<sup>15,24</sup> Briefly, the depth of the cartilage damage as well as the extent of the damaged surface was scored in a blinded manner at two different locations in the rat knee joint, i.e. the lateral and medial tibial articular cartilage. The OA score

was defined as the product of the multiplication of these two scores. The mean OA score was calculated using the scores for the two individual locations examined by three researchers (ZY, JH, and WL).

The expression of collagen type X (Col X) in articular cartilage was detected by immunohistochemistry. Briefly, the samples ( $n = 5$ ) were incubated with primary antibodies against rabbit Col X (1:200; Abcam) and subsequently with horseradish peroxidase (HRP)-conjugated secondary antibody (1:200; Santa Cruz Biotechnology, Dallas, Texas, USA). Primary antibody was replaced with blocking solution in the negative controls. The sections were examined under light microscopy. ImageJ (NIH, Bethesda, Maryland, USA) was introduced to analyze the Col X-positive area in the articular cartilage.

**Statistical analysis.** Data were analyzed with SPSS 16.0 (SPSS, Chicago, Illinois, USA). The data were presented as means and SDs. Data from qRT-PCR comparing the expression level, Rosette assay, SA- $\beta$ -Gal assay in MSCs, and M-MSCs were analyzed by independent-samples  $t$ -test. OA score in animal study was compared using Kruskal-Wallis test with Dunn's post test. Data from animal study except for OA score were analyzed by one-way analysis of variance (ANOVA) followed by post hoc multiple comparison tests (Tukey's test when equal variance was assumed, or Games-Howell test when equal

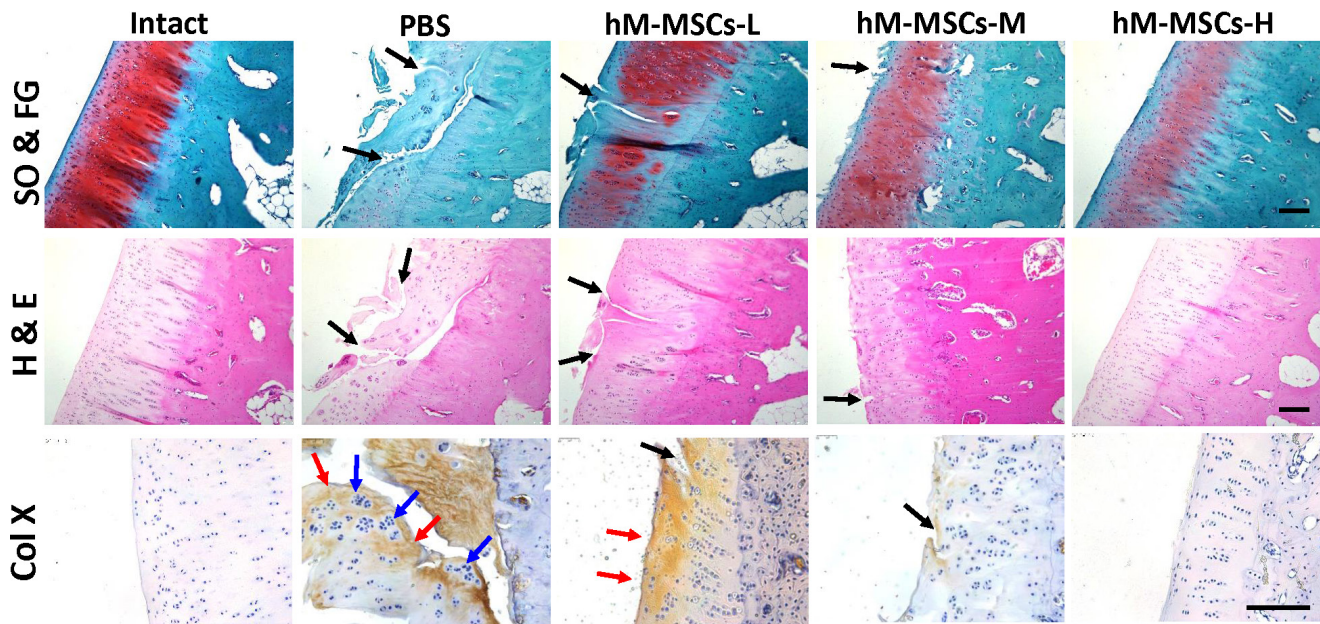


Fig. 5

The therapeutic effects of phosphate-buffered saline (PBS), low dose (2 million, hM-MSCs-L), medium dose (4 million, hM-MSCs-M), or high dose (8 million, hM-MSCs-H) of hM-MSCs on articular cartilage in the anterior cruciate ligament transection (ACLT)-induced osteoarthritis (OA) rabbits ( $n = 5$ ). The proximal tibial samples were decalcified and stained with Safranin O & Fast Green (SO & FG), haematoxylin & eosin (H & E), or anti-rabbit collagen type X (Col X) antibody. Black arrows point to the erosion and destruction of articular cartilage; blue arrows point to the clusters of chondrocytes; red arrows point to the areas of Col X positive expression in OA cartilage. Scale bar: 100  $\mu\text{m}$ . hM-MSCs, manipulated human mesenchymal stem cells.

variance was not assumed). A  $p$ -value  $< 0.05$  was considered significant.

## Results

**Cell morphology and proliferation capacity.** We successfully isolated hMSCs from the three donors. However, only two of the donors were included in our study as the cells isolated from one of the donors was not sufficiently capable during expansion to produce enough cells. Representative images from one of the donors are shown in the results, and those from the other donor are presented in the Supplementary Material. Before the experiments, the purity of hMSCs was determined by flow cytometry and lineages differentiation potential including osteogenesis, adipogenesis, and chondrogenesis as previously described.<sup>20</sup> Cell morphology and proliferation of hM-MSCs at passage 1 (p1) or 5 (p5) and their hMSCs controls (p4 or p9) are shown in Figure 1 and Supplementary Figure a. The hM-MSCs at passage 1 (hM-MSCs p1) displayed a spindle shape as well as hMSC controls (hMSCs p4) at their early passage (Figure 1a and Supplementary Figure a). However, the size of hMSCs controls (hMSCs p9) expanded at their later passage, and cell density was lower than the spindle-shaped hM-MSCs (hM-MSCs p5) (Figure 1a and Supplementary Figure a). Results from cell proliferation assay showed that hM-MSCs at early passage (hM-MSCs p1) exhibited an advantage of proliferation, increasing by 29.31% ( $p = 0.051$ , independent-samples  $t$ -test) or 30.70% ( $p = 0.016$ ,

independent-samples  $t$ -test) after 24 hours or 48 hours culture compared with hMSC controls (Figure 1b). However, there was no significant difference in cell proliferation at later passage between hM-MSCs (hM-MSCs p5) and hMSCs controls (hMSCs p9) (Figure 1c).

**Chondrogenic differentiation capacity.** After preconditioning, hM-MSCs exhibited a higher capacity of chondrogenic differentiation potential compared with the untreated hMSCs controls at early passage. From the results of Safranin O staining, we can see that hM-MSCs pellets (hM-MSCs p1) displayed more extracellular matrix (ECM) deposition and bigger size than MSCs controls (hMSCs p4) (Figure 2a and Supplementary Figure b). At later passage, however, the superior chondrogenic differentiation potential of hM-MSCs (hM-MSCs p5) was diminished, exhibiting less ECM deposition than the early passage (hM-MSCs p1) (Figure 2a). Data from qPCR presented upregulation in the expression of chondrogenic markers in hM-MSCs p1, with 79.8% ( $p = 0.052$ , independent-samples  $t$ -test), 219.4% ( $p < 0.001$ , independent-samples  $t$ -test), and 109.2% ( $p = 0.021$ , independent-samples  $t$ -test) higher in Sox9, Col2a1, and Aggrecan than the hMSC controls (hMSCs p4), respectively (Figure 2b).

**Immunogenicity.** Immune response shown by the physical interaction between human peripheral blood lymphocytes (hPBLs) and hM-MSCs was tested by Rosette assay. Interestingly, results showed that hPBLs have a higher binding affinity for untreated hMSCs both at early and late passage, as seen by the typical ring-like rosettes formed

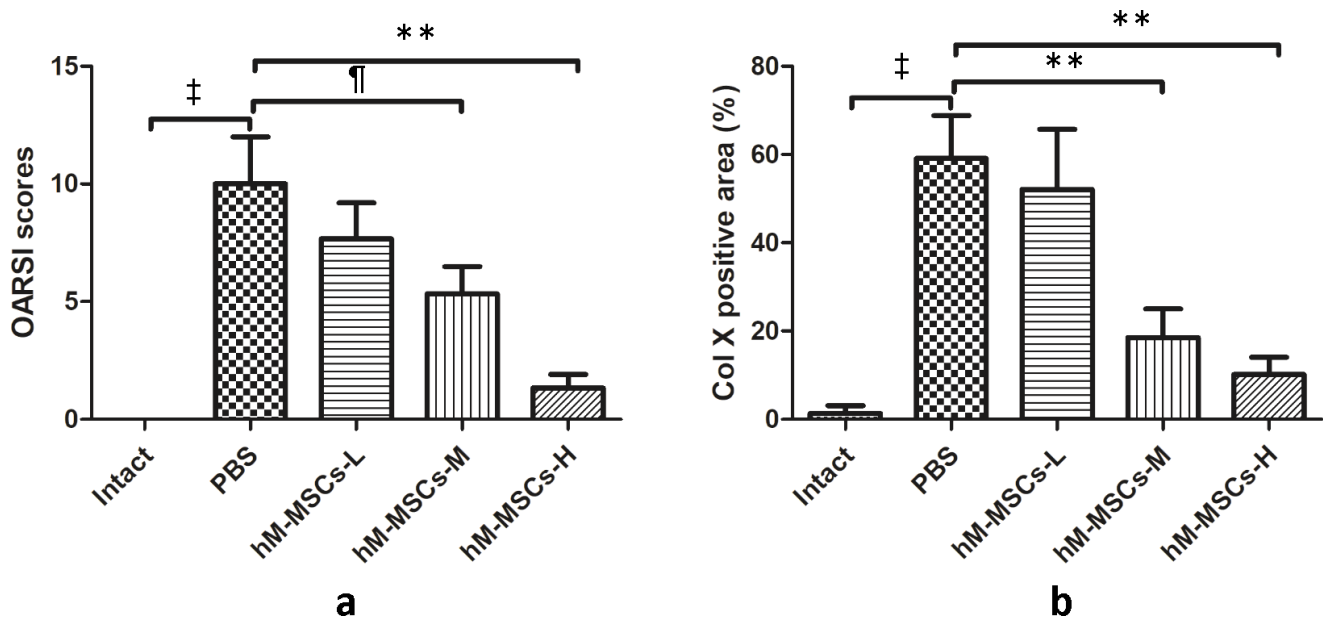


Fig. 6

Quantitative Osteoarthritis Research Society International (OARSI) score<sup>24</sup> and semi-quantitative data of the positive expression of collagen type X (Col X) in articular cartilage after treated with phosphate-buffered saline (PBS) or low dose (2 million, hM-MSCs-L), medium dose (4 million, hM-MSCs-M), or high dose (8 million, hM-MSCs-H) of hM-MSCs in the anterior cruciate ligament transection (ACL)-induced osteoarthritis (OA) rabbits (n = 5). a) OARSI score indicates the therapeutic effect of cell therapy. b) The ratio of Col X-positive expressed area in articular cartilage. Data are presented as mean and SD. †p < 0.05, †p < 0.01, ‡p < 0.001 versus Intact; \*p < 0.01, \*\*p < 0.001 versus PBS group. hM-MSCs, manipulated human mesenchymal stem cells.

around untreated hMSCs by fluorescent microscope (Figure 3a and Supplementary Figure c). Quantitative results showed a significantly higher hPBL binding ratio in hMSCs than hM-MSCs (42.2% vs 22.9% in p1, p = 0.014, independent-samples *t*-test; 69.0% vs 35.4% in p5, p = 0.001, independent-samples *t*-test) (Figure 3b).

**Senescence.** Cell senescence was determined by their cellular level of  $\beta$ -galactosidase activity. Results showed that none of the early-passage hMSCs (hMSCs p4) or hM-MSCs (hM-MSCs p1) stained positively for SA- $\beta$ -gal activity (Figures 4a and Supplementary Figure d). Although many hMSCs controls (hMSCs p9) stained positively for SA- $\beta$ -gal activity at late passage, very few hM-MSCs (hM-MSCs p5) were positively stained (Figures 4a and Supplementary Figure d). Enzymatic activity assays in cell lysate also demonstrated very low  $\beta$ -galactosidase activity in early passage of hMSCs (p4) or hM-MSCs (p1), whereas the late passage hMSCs (p9) controls displayed a higher level of SA- $\beta$ -gal activity compared with hM-MSCs (p5) (2.43 vs 0.49, p = 0.007, independent-samples *t*-test) (Figure 4b).

**Cell therapy outcomes.** To determine the acute response of cell therapy, local temperature of the affected knee skin was monitored before and after cell therapy. As shown in Supplementary Figure ea, local temperature rose gradually until approximately 40°C at 14 days postoperatively. The temperature then gradually decreased after cell therapy to around 38°C at 30 days after cell injections, regardless of the number of cells injected (Supplementary Figure eb).

To evaluate the efficacy of cell therapy on a surgically induced OA rabbit model, pathological changes in the affected knee joints were measured by histological analysis and micro-CT analysis. Compared with the contralateral intact controls, the PBS-treated group showed remarkable OA-like phenotypes such as cartilage erosion or destruction, as indicated by the gross view of the tibial plateau (Supplementary Figure f), histological staining results, and the significantly higher OA scores (10.0 vs 0, p = 0.000, ANOVA) (Figures 5 and 6a). Data from immunohistochemistry also showed that highly expressing Col X (59.08% in PBS group vs 1.40% in intact controls, p = 0.000, ANOVA), and increasing numbers and sizes of chondrocyte clusters were found in the PBS-treated group (Figures 5 and 6b). Manipulated hMSCs exhibited different therapeutic effect on OA progression, depending on the cell numbers given to the rabbits. When treated with low (two million) or medium (four million) numbers of hM-MSCs, we found vertical fissures or discontinuous surface and a small amount of Col X expression in the cartilage (Figure 6a and b). However, when treated with the highest number (eight million) of hM-MSCs, the cartilage surface was quite smooth and the expression of Col X was much lower (10.20% in hM-MSCs-H group vs 59.08% in PBS group, p = 0.000, ANOVA), as also indicated by lower OA scores (1.3 in hM-MSCs-H group vs 10.0 in PBS group, p = 0.000, ANOVA) (Figure 6a and b). Interestingly, we found that cartilage damage mainly happened on the medial side of the OA joints in rabbits. Data showed higher OA scores



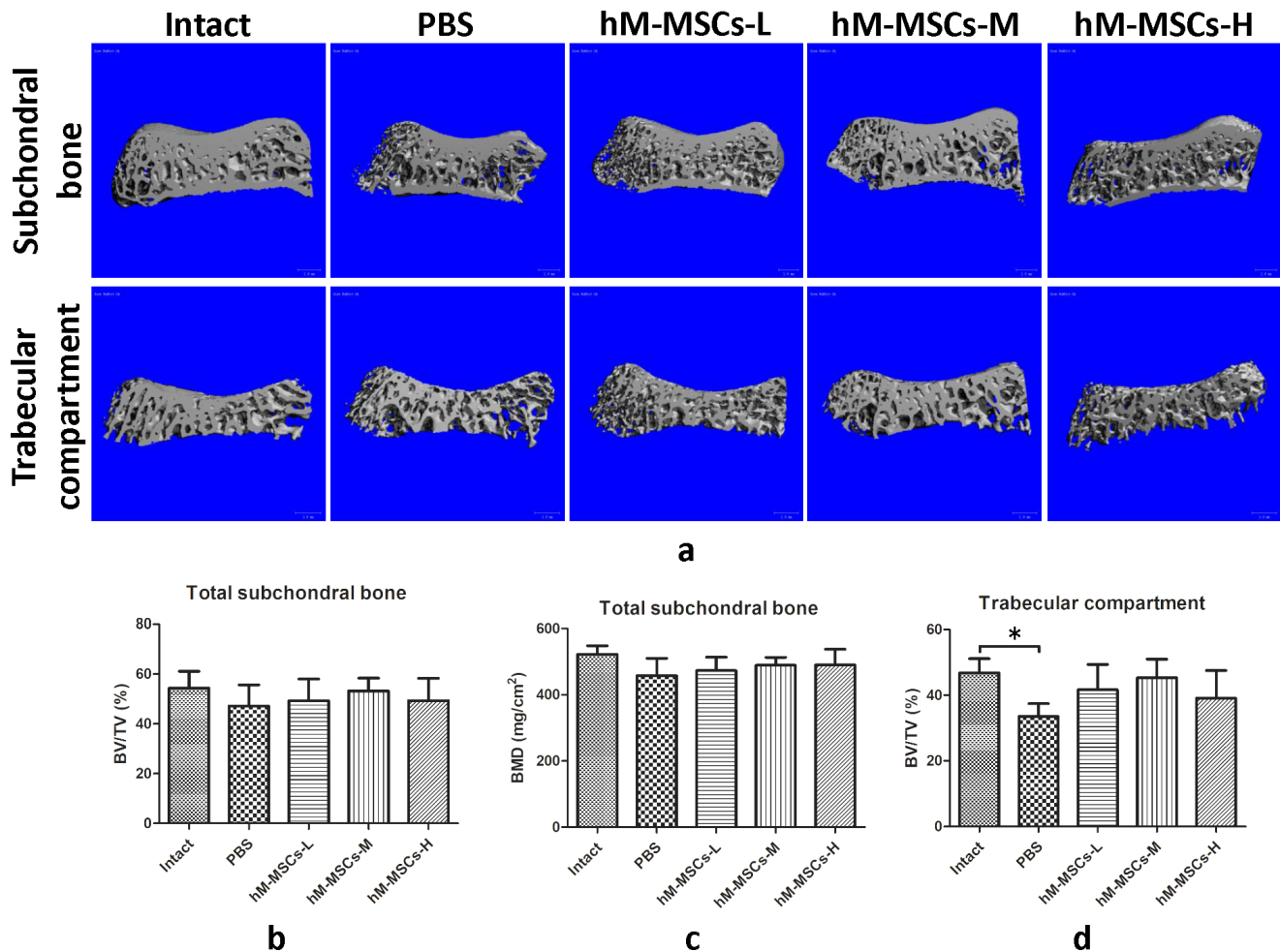


Fig. 7

Microstructural changes of subchondral bone of tibial condyles after treated with phosphate-buffered saline (PBS) or low dose (2 million, hM-MSCs-L), medium dose (4 million, hM-MSCs-M), or high dose (8 million, hM-MSCs-H) of hM-MSCs in the anterior cruciate ligament transection (ACLT)-induced osteoarthritis (OA) rabbits ( $n = 5$ ). a) 3D images of microstructure of subchondral bone and their trabecular compartment. b) Bone volume fraction (bone volume/tissue volume (BV/TV) or c) bone mineral density (BMD) of microstructure of subchondral bone and d) their trabecular compartment. Data are presented as mean and SD. \* $p < 0.05$  versus Intact.

on the medial side compared with those on the lateral side in either the PBS-treated group or cell-treated groups (Supplementary Figure g). Histological results of synovial tissue revealed no significant inflammation in all the samples (Supplementary Figure h). Results of micro-CT analysis showed no significant changes in microstructure of total subchondral bone, but a significant decrease in bone volume fraction (46.81% vs 33.51% in BV/TV,  $p = 0.035$ , ANOVA) in the trabecular compartment was observed in subchondral bone of the PBS-treated OA rabbits (Figure 7a and 7d).

## Discussion

Stem cell-based therapy has become a novel alternative treatment for tissue regeneration due to its self-renewal ability, and anti-inflammatory and immunomodulatory capacity.<sup>25,26</sup> Many preclinical or clinical studies have successfully indicated the benefit of intra-articular injection of MSCs on improvement in joint function, though

results have been inconsistent on cartilage restoration. MSCs may play different roles in OA treatment depending on the different pathological stage of subjects. For very early stages of traumatic OA, local administration of MSCs may mainly contribute to the regeneration of cartilaginous tissues like meniscus. Murphy et al<sup>27</sup> report that local delivery of bone marrow MSCs in a surgically induced caprine model stimulates regeneration of meniscal tissue and retards the progressive destruction of articular cartilage. This result is in line with previous findings that synovial stem cells or bone marrow-derived MSCs can differentiate directly into meniscal cells and promote meniscus regeneration in a surgically induced OA rat model.<sup>15,28</sup> For later stages of OA, however, MSC therapy may mainly contribute to the anti-inflammatory and immunomodulatory effects on the microenvironment of OA joints, but not restoration of cartilage. Increasingly, evidence indicates that the engraftment of injected or implanted MSCs at the damaged sites was much smaller

than expected.<sup>29</sup> The bioactive paracrine factors secreted by MSCs may play a dominant role in modulating the microenvironment of the damaged joints, leading to more favourable conditions for cartilage regeneration.<sup>30</sup> However, the cellular status has a great impact on their proliferation, regeneration, or anti-inflammatory and immunomodulatory properties. Ageing- or replicative senescence-related decline in cellular proliferation and regeneration potential is the most common obstacle of MSC-based therapy.<sup>31</sup>

Ageing-associated regenerative decline is attributed to age-related dysfunction in tissue-specific adult stem cells throughout the body. Therefore, improving adult stem cell function provides a potential approach for rejuvenating regenerative capacity. Many exciting advancements have been made in terms of rejuvenating adult stem cells. Parabiosis experiments that connect the circulatory systems of young and old mice have revealed circulating protein growth differentiation factor 11 (GDF11) in young blood is a rejuvenating factor for skeletal muscle stem cells and neural stem cells.<sup>32,33</sup> Human platelet lysate was also found to be effective in rejuvenating MSCs proliferation and differentiation, with better effects from younger donor.<sup>34,35</sup> It was also reported that treatment with the nicotinamide adenine dinucleotide (NAD(+)) precursor nicotinamide riboside (NR) rejuvenates intestinal stem cells from aged mice and reverses an impaired ability to repair gut damage.<sup>36</sup> Fasting, or the fasting mimetic metformin, was recently reported to show potential in rejuvenating poor remyelination in aged stem cells in rodents, reversing ageing changes and restoring the regenerative capacity.<sup>37</sup>

Many preconditioning approaches have been reported to rejuvenate adult stem cell proliferation and chondrogenic potential, including hypoxia, cytokines, growth factors, and genetic manipulation.<sup>38</sup> In the current study, although the cellular functions of MSCs isolated from ageing donors have not been compared with younger donors, cell proliferation, cell morphology, and chondrogenic potential exhibited incompetence. We further proved that the proliferation and chondrogenic differentiation potential of MSCs from ageing donors could be greatly enhanced after stepwise preconditioning in the chondrogenic medium and normal growth medium. These results, as well as previous findings, indicate a rejuvenation effect on cell proliferation and differentiation of the preconditioning methods, even in cells from ageing donors.<sup>15,16</sup> The possible underlying mechanism is epigenetic modification in the pluripotent markers, which further enhances the multipotency of the MSCs.<sup>15</sup> Although there was a superior proliferation and chondrogenic differentiation potential in early passage hM-MSCs (p1), we observed a decline trend in the proliferation and chondrogenic differentiation potential in both of hMSCs and hM-MSCs after five passages, indicating replicative senescence in those later passage cells. For stem cell-based OA therapy, a large amount of MSCs are essential

to achieve a therapeutic effect. It is critical to achieve expansion without compromising differentiation potential, or anti-inflammatory or immunomodulatory properties. However, after long-term ex vivo culture (43 to 77 days of cultivation, or seven to 12 passages), MSCs present replicative senescence, which is characterized by proliferation arrest and differentiation deficiency.<sup>14</sup> Interestingly, from the data  $\beta$ -Gal assays, we observed hM-MSCs were more resistant to senescence at later passage. However, since the advantages in proliferation and differentiation of hM-MSCs are due to the epigenetic modification in pluripotent genes during stepwise preconditioning, these are prone to diminish gradually after long-term culture. In a clinical setting, it would be of value to use the cells in their early passages.

MSCs have long been regarded as hypoimmunogenic or immune privileged.<sup>39</sup> This property enables MSC transplantation across major histocompatibility complex (MHC) barriers. However, recent evidence showing the generation of antibodies against and immune rejection of allogenic MSCs suggests that they may not actually be immune privileged.<sup>40</sup> Interestingly, from our cellular data we found not only that senescence, but also immunogenicity could be statistically significantly enhanced after another five passages in untreated hMSCs rather than hM-MSCs (p5). Recent evidence showed that the cells that underwent senescence appeared to promote an immunogenic phenotype that facilitates self-elimination by the immune system.<sup>41</sup> The senescent cells may secrete proinflammatory cytokines which can attract and activate immune cells. Furthermore, upregulation of membrane-bound immune ligands allows for specific recognition, and promiscuous gene expression may generate an array of tissue-restricted proteins that could subsequently be processed into peptides for presentation via MHC molecules.<sup>41</sup> Taken together, based on the current cellular data, we found that hM-MSCs showed many advantages of hMSCs in higher cell proliferation and chondrogenic differentiation, but lower immunogenicity and senescence after ex vivo culture, indicating a better clinical implication in OA treatment.

In the preclinical rabbit OA model, we found cartilage damage happened mainly on the medial side of the tibial plateau of the affected rabbit joints after ACL transection. Previous studies also provided similar evidence in human samples.<sup>42,43</sup> We have not found any significant difference in BV/TV of the total subchondral bone in OA rabbits compared with intact controls. Interestingly, we found significant bone loss at the trabecular bone in the OA rabbits after segregating the trabecular bone from the total subchondral bone. Subchondral bone remodelling during OA development could be a dynamic pathological process. It was reported that bone remodelling could be accelerated at early stage of OA, resulting in bone loss at this early stage.<sup>44</sup> Then the subchondral plate would harden at late stage.<sup>44</sup> Manipulated hMSCs showed various therapeutic outcomes depending on the cell

numbers applied, with better outcomes in higher dose groups. As shown by the histological results, hM-MSCs effectively retarded the progressive destruction of articular cartilage. Meanwhile, 3D imaging results revealed a preventive effect on subchondral bone remodelling in the affected tibia. Local temperature profile measured after cell injection and synovial tissue histology showed no pathological change after treatment of hM-MSCs. The overall results in the rabbit OA model are consistent with the previous findings from the rat OA model of Lin et al,<sup>15</sup> providing a safe and efficient approach for OA therapy. In this study, cell therapy was performed after 14 days of ACL transection in the rabbits without removal of medial meniscus, which was removed in the rat models.<sup>15,28</sup> The injected hM-MSCs at this early stage may be primarily involved in maintaining the cartilaginous tissue, with senescence resistance and immune privilege. Meanwhile, as high concentration of proinflammatory factor or chemokine presented in such early stage after cartilage injury, hM-MSCs may also play an important role in inflammation modulation by regulating the activity of immunocytes including T cells, B cells, and NK cells through various pathways and direct cell contact.<sup>45–47</sup> Hence, the results revealed that xenogeneic transplantation of hMSCs in rabbits could be safe and effective, which is consistent with previous reports.<sup>48,49</sup>

However, there are still some limitations in this study. First, in the cellular study, we didn't include younger donors to compare the functions between cells isolated from young and ageing donors, and to define the ageing changes in cellular behaviour. Second, in the animal study, we did not investigate the effect of hMSCs in the OA rabbits; the mechanisms of such modulation effects of cell therapy in the process of cartilage protection have not been elucidated.

Overall, our study demonstrated a reliable and feasible preconditioning strategy to rejuvenate stemness of adult MSCs with lower senescence and immunogenicity. We also verified the enhanced safety and efficacy of the resulting cells in cartilage restoration, which may shed light on a further clinical translation of stem cell-based OA therapy.

### Supplementary material



Supplementary figures show the cellular results from the other donors and supplementary data from the animal study.

### References

- Brooks PM. Impact of osteoarthritis on individuals and society: how much disability? social consequences and health economic implications. *Curr Opin Rheumatol*. 2002;14(5):573–577.
- Lawrence RC, Felson DT, Helmick CG, et al. Estimates of the prevalence of arthritis and other rheumatic conditions in the United States. Part II. *Arthritis Rheum*. 2008;58(1):26–35.
- Symonds T, Hughes B, Liao S, Ang Q, Bellamy N. Validation of the Chinese Western Ontario and McMaster universities osteoarthritis index in patients from mainland China with osteoarthritis of the knee. *Arthritis Care Res*. 2015;67(11):1553–1560.
- Nelson AE, Allen KD, Golightly YM, Goode AP, Jordan JM. A systematic review of recommendations and guidelines for the management of osteoarthritis: the chronic osteoarthritis management initiative of the U.S. bone and joint initiative. *Semin Arthritis Rheum*. 2014;43(6):701–712.
- León SA, Mei XY, Safir OA, Gross AE, Kuzyk PR. Long-Term results of fresh osteochondral allografts and realignment osteotomy for cartilage repair in the knee. *Bone Joint J*. 2019;101-B(1\_Suppl\_A):46–52.
- Shi D, Clement ND, Bhone R, et al. Society for translational medicine-expert consensus on the treatment of osteoarthritis. *Ann Jt*. 2019;4(September):1–12.
- Peterson L, Vasiliadis HS, Brittberg M, Lindahl A. Autologous chondrocyte implantation: a long-term follow-up. *Am J Sports Med*. 2010;38(6):1117–1124.
- Schnabel M, Marlovits S, Eckhoff G, et al. Dedifferentiation-associated changes in morphology and gene expression in primary human articular chondrocytes in cell culture. *Osteoarthritis Cartilage*. 2002;10(1):62–70.
- Lee WY-W, Wang B. Cartilage repair by mesenchymal stem cells: clinical trial update and perspectives. *J Orthop Translat*. 2017;9:76–88.
- Kong L, Zheng L-Z, Qin L, Ho KKW. Role of mesenchymal stem cells in osteoarthritis treatment. *J Orthop Translat*. 2017;9:89–103.
- Mahmoud EE, Adachi N, Mawas AS, Deie M, Ochi M. Multiple intra-articular injections of allogeneic bone marrow-derived stem cells potentially improve knee lesions resulting from surgically induced osteoarthritis: an animal study. *Bone Joint J*. 2019;101-B(7):824–831.
- Roobrouck VD, Ulloa-Montoya F, Verfaillie CM. Self-Renewal and differentiation capacity of young and aged stem cells. *Exp Cell Res*. 2008;314(9):1937–1944.
- Steinert AF, Ghivizzani SC, Rethwilm A, Tuan RS, Evans CH, Nöth U. Major biological obstacles for persistent cell-based regeneration of articular cartilage. *Arthritis Res Ther*. 2007;9(3):213.
- Wagner W, Horn P, Castoldi M, et al. Replicative senescence of mesenchymal stem cells: a continuous and organized process. *PLoS One*. 2008;3(5):e2213.
- Lin S, Lee WY-W, Xu L, et al. Stepwise preconditioning enhances mesenchymal stem cell-based cartilage regeneration through epigenetic modification. *Osteoarthritis Cartilage*. 2017;25(9):1541–1550.
- Lin S, Lee WY-W, Feng Q, et al. Synergistic effects on mesenchymal stem cell-based cartilage regeneration by chondrogenic preconditioning and mechanical stimulation. *Stem Cell Res Ther*. 2017;8(1):221.
- World Medical Association. World Medical association Declaration of Helsinki: ethical principles for medical research involving human subjects. *JAMA*. 2013;310(20):2191–2194.
- García-Álvarez F, Alegre-Aguarón E, Desportes P, et al. Chondrogenic differentiation in femoral bone marrow-derived mesenchymal cells (MSC) from elderly patients suffering osteoarthritis or femoral fracture. *Arch Gerontol Geriatr*. 2011;52(2):239–242.
- Filardo G, Petretta M, Cavallo C, et al. Patient-Specific meniscus prototype based on 3D bioprinting of human cell-laden scaffold. *Bone Joint Res*. 2019;8(2):101–106.
- Wang B, Lee WY-W, Huang B, et al. Secretome of human fetal mesenchymal stem cell ameliorates replicative senescence. *Stem Cells Dev*. 2016;25(22):1755–1766.
- Chen X, McClurg A, Zhou G-Q, McCaigue M, Armstrong MA, Li G. Chondrogenic differentiation alters the immunosuppressive property of bone marrow-derived mesenchymal stem cells, and the effect is partially due to the upregulated expression of B7 molecules. *Stem Cells*. 2007;25(2):364–370.
- Lee BY, Han JA, Im JS, et al. Senescence-Associated beta-galactosidase is lysosomal beta-galactosidase. *Aging Cell*. 2006;5(2):187–195.
- Zhen G, Wen C, Jia X, et al. Inhibition of TGF- $\beta$  signaling in mesenchymal stem cells of subchondral bone attenuates osteoarthritis. *Nat Med*. 2013;19(6):704–712.
- Pritzker KPH, Gay S, Jimenez SA, et al. Osteoarthritis cartilage histopathology: grading and staging. *Osteoarthritis Cartilage*. 2006;14(1):13–29.
- Murphy MB, Moncivais K, Caplan AI. Mesenchymal stem cells: environmentally responsive therapeutics for regenerative medicine. *Exp Mol Med*. 2013;45(11):e54.
- Schmalzl J, Plumbhoff P, Gilbert F, et al. Tendon-Derived stem cells from the long head of the biceps tendon: inflammation does not affect the regenerative potential. *Bone Joint Res*. 2019;8(9):414–424.
- Murphy JM, Fink DJ, Hunziker EB, Barry FP. Stem cell therapy in a caprine model of osteoarthritis. *Arthritis Rheum*. 2003;48(12):3464–3474.
- Horie M, Sekiya I, Muneta T, et al. Intra-Articular injected synovial stem cells differentiate into mesenchymal cells directly and promote meniscal regeneration without mobilization to distant organs in rat massive meniscal defect. *Stem Cells*. 2009;27(4):878–887.
- Granero-Molto F, Weis JA, Longobardi L, Spagnoli A. Role of mesenchymal stem cells in regenerative medicine: application to bone and cartilage repair. *Expert Opin Biol Ther*. 2008;8(3):255–268.



30. **Wu L, Leijten JCH, Georgi N, Post JN, van Blitterswijk CA, Karperien M.** Trophic effects of mesenchymal stem cells increase chondrocyte proliferation and matrix formation. *Tissue Eng Part A*. 2011;17(9-10):1425–1436.
31. **Zong Z, Wu X, Su Z, et al.** Cartilage Tissue Engineering : An Update on Multi-Component Approach. *Journal of Orthopaedic and Rheumatology*. 2019;6(1):1–7.
32. **Sinha M, Jang YC, Oh J, et al.** Restoring systemic Gdf11 levels reverses age-related dysfunction in mouse skeletal muscle. *Science*. 2014;344(6184):649–652.
33. **Katsimpardi L, Litterman NK, Schein PA, et al.** Vascular and neurogenic rejuvenation of the aging mouse brain by young systemic factors. *Science*. 2014;344(6184):630–634.
34. **Griffiths S, Baraniak PR, Copland IB, Nerem RM, McDevitt TC.** Human platelet lysate stimulates high-passage and senescent human multipotent mesenchymal stromal cell growth and rejuvenation in vitro. *Cytotherapy*. 2013;15(12):1469–1483.
35. **Lohmann M, Walenda G, Hemeda H, et al.** Donor age of human platelet lysate affects proliferation and differentiation of mesenchymal stem cells. *PLoS One*. 2012;7(5):e37839–6.
36. **Igarashi M, Miura M, Williams E, et al.** NAD<sup>+</sup> supplementation rejuvenates aged gut adult stem cells. *Aging Cell*. 2019;18(3):e12935–10.
37. **Neumann B, Baror R, Zhao C, et al.** Metformin restores CNS remyelination capacity by Rejuvenating aged stem cells. *Cell Stem Cell*. 2019;25(4):473–485.
38. **Pei M.** Environmental preconditioning rejuvenates adult stem cells' proliferation and chondrogenic potential. *Biomaterials*. 2017;117:10–23.
39. **Shi Y, Su J, Roberts AI, Shou P, Rabson AB, Ren G.** How mesenchymal stem cells interact with tissue immune responses. *Trends Immunol*. 2012;33(3):136–143.
40. **Ankrum JA, Ong JF, Karp JM.** Mesenchymal stem cells: immune evasive, not immune privileged. *Nat Biotechnol*. 2014;32(3):252–260.
41. **Burton DGA, Faragher RGA.** Cellular senescence: from growth arrest to immunogenic conversion. *Age*. 2015;37(2):1–19.
42. **Chou C-H, Lee MTM, Song I-W, et al.** Insights into osteoarthritis progression revealed by analyses of both knee tibiofemoral compartments. *Osteoarthritis Cartilage*. 2015;23(4):571–580.
43. **Sanjurjo-Rodriguez C, Baboolal TG, Burska AN, et al.** Gene expression and functional comparison between multipotential stromal cells from lateral and medial condyles of knee osteoarthritis patients. *Sci Rep*. 2019;9(1):1–12.
44. **Burr DB, Gallant MA.** Bone remodelling in osteoarthritis. *Nat Rev Rheumatol*. 2012;8(11):665–673.
45. **Najar M, Raicevic G, Boufker HI, et al.** Mesenchymal stromal cells use PGE2 to modulate activation and proliferation of lymphocyte subsets: combined comparison of adipose tissue, Wharton's jelly and bone marrow sources. *Cell Immunol*. 2010;264(2):171–179.
46. **Le Blanc K, Davies LC.** Mesenchymal stromal cells and the innate immune response. *Immunol Lett*. 2015;168(2):140–146.
47. **Siegel G, Schäfer R, Dazzi F.** The immunosuppressive properties of mesenchymal stem cells. *Transplantation*. 2009;87(9 Suppl):S45–S49.
48. **Lin C-S, Lin G, Lue TF.** Allogeneic and xenogeneic transplantation of adipose-derived stem cells in immunocompetent recipients without immunosuppressants. *Stem Cells Dev*. 2012;21(15):2770–2778.
49. **Henriksson HB, Svanvik T, Jonsson M, et al.** Transplantation of human mesenchymal stem cells into intervertebral discs in a xenogeneic porcine model. *Spine*. 2009;34(2):141–148.

**Author information:**

- Z. Zong, MD, Postgraduate Student
- T. Chen, Undergraduate Student
- J. Yu, Undergraduate Student

- J. Chen, MD, Associate Consultant
- B. Wei, MD, Professor  
Orthopaedic Center, Affiliated Hospital of Guangdong Medical University, First Clinical Medical College, Guangdong Medical University, Zhanjiang, China.
- X. Zhang, MSc, PhD Student
- Z. Yang, MSc, Postgraduate Student
- W. Lin, PhD, Postdoctoral Fellow
- G. Li, MBBS, D. Phil, Professor  
Department of Orthopaedics and Traumatology, Faculty of Medicine, The Chinese University of Hong Kong, Hong Kong, Hong Kong; Stem Cells and Regenerative Medicine Laboratory, Li Ka Shing Institute of Health Sciences, The Chinese University of Hong Kong, Prince of Wales Hospital, Hong Kong, Hong Kong.
- W. Yuan, BS, Postgraduate Student, Department of Biomedical Engineering, Faculty of Engineering, Chinese University of Hong Kong, Hong Kong, Hong Kong.
- J. Huang, DDS, Associate Consultant, Department of Stomatology, Second Clinical Medical College, Guangdong Medical University, Dongguan, China.
- L. Cui, PhD, Professor, Department of Pharmacology, The Public Service Platform of South China Sea for R&D Marine Biomedicine Resources, Marine Biomedical Research Institute, Guangdong Medical University, Zhanjiang, China.
- S. Lin, MD, PhD, Associate Professor, Orthopaedic Center, Affiliated Hospital of Guangdong Medical University, First Clinical Medical College, Guangdong Medical University, Zhanjiang, China; Department of Pharmacology, The Public Service Platform of South China Sea for R&D Marine Biomedicine Resources, Marine Biomedical Research Institute, Guangdong Medical University, Zhanjiang, China; Department of Orthopaedic Surgery, School of Medicine, Stanford University, Stanford, USA.

**Author contributions:**

- Z. Zong: Carried out the cellular and animal studies, Wrote the manuscript.
- X. Zhang: Carried out the cellular and animal studies.
- Z. Yang: Conducted the sample processing, histological staining, and scoring.
- W. Yuan: Provided the materials, human samples, and methodology.
- J. Huang: Conducted the sample processing, histological staining, and scoring.
- W. Lin: Conducted the sample processing, histological staining, and scoring.
- T. Chen: Carried out the animal care.
- J. Yu: Carried out the animal care.
- J. Chen: Provided the materials, human samples, and methodology.
- L. Cui: Provided advice regarding the study design and data analysis.
- G. Li: Provided advice regarding the study design and data analysis.
- B. Wei: Harvested human samples and provided the funding and supervision.
- S. Lin: Provided the funding and supervision.

■ Z. Zong and X. Zhang contributed equally to this work.

■ Z. Zong and X. Zhang are co-first authors.

**Funding statement:**

- This study was supported by National Natural Science Foundation of China (81874000), Natural Science Foundation of Guangdong Province Science and Technology Department (2018A030313374 and 2019A1515110724), Hong Kong Government Research Grant Council, and General Research Fund (14120118 and T13-402/17-N). This study was also partially supported by the funds from Stem Cell Preclinical Research Projects of the Affiliated Hospital of Guangdong Medical University (2018PSSC001), Science and technology fund of Zhanjiang (171113211683046), open fund from Marine Biomedical Research Institute, Guangdong Medical University, and Peaking Plan of the Affiliated Hospital of Guangdong Medical University. No benefits in any form have been received or will be received from a commercial party related directly or indirectly to the subject of this article.

**Acknowledgements**

- We thank X. Wu, Z. Zhao, Z. Wang, and Z. Su for helping in animal care and surgeries. We also thank Dr. Alex Stahl for the help in language editing.

**Ethical review statement**

- The study was carried out in accordance with The Code of Ethics of the World Medical Association (Declaration of Helsinki) for experiments involving humans. Procedures involved in cell harvesting and culturing were approved by Clinical Research Ethical Committee of Affiliated Hospital of Guangdong Medical University, and informed consent from the patients was obtained before experiments.

© 2021 Author(s) et al. This is an open-access article distributed under the terms of the Creative Commons Attribution Non-Commercial No Derivatives (CC BY-NC-ND 4.0) licence, which permits the copying and redistribution of the work only, and provided the original author and source are credited. See <https://creativecommons.org/licenses/by-nc-nd/4.0/>.